

FAK Potentiates Rac1 Activation and Localization to Matrix Adhesion Sites: A Role for β PIX[□]

Fumin Chang,* Christopher A. Lemmon,*[†] Dongeun Park,[‡]
and Lewis H. Romer*^{S||}

Departments of *Anesthesiology and Critical Care Medicine, [†]Biomedical Engineering, ^SCell Biology, and ^{||}Pediatrics, Johns Hopkins University School of Medicine, Baltimore, MD 21287; and [‡]School of Biological Sciences, Seoul National University, Seoul 151-742, South Korea

Submitted March 17, 2006; Revised October 25, 2006; Accepted October 27, 2006

Monitoring Editor: Carole Parent

FAK, a cytoplasmic protein tyrosine kinase, is activated and localized to focal adhesions upon cell attachment to extracellular matrix. FAK null cells spread poorly and exhibit altered focal adhesion turnover. Rac1 is a member of the Rho-family GTPases that promotes membrane ruffling, leading edge extension, and cell spreading. We investigated the activation and subcellular location of Rac1 in FAK null and FAK reexpressing fibroblasts. FAK reexpressers had a more robust pattern of Rac1 activation after cell adhesion to fibronectin than the FAK null cells. Translocation of Rac1 to focal adhesions was observed in FAK reexpressers, but seldom in FAK null cells. Experiments with constitutively active L61Rac1 and dominant negative N17Rac1 indicated that the activation state of Rac1 regulated its localization to focal adhesions. We demonstrated that FAK tyrosine-phosphorylated β PIX and thereby increased its binding to Rac1. In addition, β PIX facilitated the targeting of activated Rac1 to focal adhesions and the efficiency of cell spreading. These data indicate that FAK has a role in the activation and focal adhesion translocation of Rac1 through the tyrosine phosphorylation of β PIX.

INTRODUCTION

Integrin receptors are activated and clustered at sites of extracellular matrix (ECM) binding, leading to the tyrosine phosphorylation of a number of downstream signaling proteins including FAK (Hanks *et al.*, 1992; Schaller *et al.*, 1992; Romer *et al.*, 2006). Autophosphorylation of FAK at Tyr-397 creates a binding site for Src. After binding to FAK, Src phosphorylates FAK on several other tyrosine residues, including Tyr-925 and Tyr-576/577 to achieve full FAK activation and scaffolding potential (Schlaepfer *et al.*, 1999; Schaller 2001). Tyr-576 and -577 are in the FAK kinase activation loop, and phosphorylation on these sites enhances catalytic activity (Ruest *et al.*, 2000). Phosphorylation on Tyr-925 induces the recruitment of Grb2 and promotes the activation of the Ras/Raf/MEK/ERK pathway (Schlaepfer *et al.*, 1997). In addition to Src, phosphorylation on FAK Tyr-397 also induces the recruitment of Shc and p130CAS to focal adhesions (Schlaepfer *et al.*, 1997; Takahashi *et al.*, 1999). Src and FAK also directly mediate the tyrosine phosphorylation of p130CAS and paxillin, leading in turn to the recruitment of Crk and Nck and the assembly of multiphosphocomponent signaling complexes at focal adhesions (Schaller and Parsons 1995; Schlaepfer *et al.*, 1999; Turner, 2000; Romer *et al.*, 2006).

FAK's role in cell spreading has been investigated since reports that FAK null fibroblasts from knockout mice exhib-

ited similar plating efficiency but poor spreading when compared with normal controls (Ilic *et al.*, 1995). Reexpression of FAK in the FAK null cells restores their ability to spread on fibronectin (Owen *et al.*, 1999; Sieg *et al.*, 1999), whereas overexpression of either the dominant negative FAK protein FRNK, or the FAK-inactivating phosphatases PTEN or Shp-2, results in delayed or impaired cell spreading (Richardson and Parsons 1996; Gu *et al.*, 1998; Yu *et al.*, 1998). FAK was once thought to be a direct catalyst for the formation of focal adhesions—anchor points for cell motility (Burridge *et al.*, 1992; Richardson *et al.*, 1997). Later it was discovered that FAK suppresses Rho activity and promotes focal adhesion turnover (Ren *et al.*, 2000; Schaller, 2001; Ezratty *et al.*, 2005).

Cell spreading is regulated by coordinated changes in integrin-mediated adhesions to ECM and reorganization of the actin cytoskeleton by Rho family GTP-binding proteins (Machesky and Hall 1997; Nobes and Hall, 1999; Clark *et al.*, 1998; Ren *et al.*, 1999; Hall, 2005). Rac1 and Cdc42 promote actin polymerization, inducing the formation of lamellipodia and filopodia respectively to drive extension of the leading cell edge. On the other hand, Rho-regulated myosin-dependent contractile force is transiently reduced by mechanisms involving Src, FAK, and the Rho inactivating protein p190RhoGAP (Ren *et al.*, 1999, 2000; Arthur *et al.*, 2000). Arthur *et al.* (2000) demonstrated that p190RhoGAP is tyrosine-phosphorylated in a Src-dependent manner, and tyrosine phosphorylation of p190RhoGAP by FAK has been shown *in vitro* by Holinstat *et al.* (2006). Thus, Src and FAK inactivate RhoA activity via p190RhoGAP after integrin-mediated adhesion. This “relaxes” cytoskeletal tension, allowing the formation of membrane extensions.

The Rho family GTPases cycle between inactive GDP-bound and active GTP-bound forms and their activation is mediated by guanine nucleotide exchange factors (GEFs; Hall, 2005). FAK interactions with Rac-activation mecha-

This article was published online ahead of print in *MBC in Press* (<http://www.molbiolcell.org/cgi/doi/10.1091/mbc.E06-03-0207>) on November 8, 2006.

□ The online version of this article contains supplemental material at *MBC Online* (<http://www.molbiolcell.org>).

Address correspondence to: Lewis Romer (Lromer@jhmi.edu).

nisms that may positively mobilize cell spreading are still incompletely understood and may proceed along multiple pathways. Thus, Hsia and coworkers showed that viral Src transformation does not fully restore Rac-dependent invasive behavior in FAK null cells. In fact, the transient accumulation of FAK at the lamellipodia of FAK-expressing fibroblasts is associated with the formation of a signaling complex with Src, p130CAS, and Dock180 and elevation of both Rac and JNK activity (Hsia *et al.*, 2003). Rac1 function is positively regulated by β PIX and is modulated by PAK. PIX (PAK-interacting exchange factor)/Cool (cloned out of library) protein was identified as a PAK-binding protein (Manser *et al.*, 1998). Overexpression of β PIX drives formation of membrane ruffles via activation of Rac1. Targets for PAK on β PIX are S525 and T526. After PAK-mediated phosphorylation, β PIX specifically localizes to lamellipodia at neuronal growth cones in response to bFGF, and mutation of both S525 and T526 to alanines causes defective lamellipodial targeting (Shin *et al.*, 2002). Shin *et al.* (2004) also showed that Rac activation induced by β PIX was increased after phosphorylation on S525 and T526 by PAK. In addition to PAK, β PIX has been shown to bind to the ArfGAP family protein paxillin kinase linker (PKL; Turner *et al.*, 1999) and to the G protein-coupled receptor kinase-interacting protein GIT-1 (Zhao *et al.*, 2000), which both interact with paxillin (Turner *et al.*, 1999; Zhao *et al.*, 2000; West *et al.*, 2001). Mechanisms of β PIX targeting and turnover at focal adhesions and the implications for Rac function are foci of intense investigation and debate (Brown *et al.*, 2002; ten Klooster *et al.*, 2006).

Our results delineate a signaling pathway directly linking FAK to Rac1 activation and Rac1-mediated cell spreading via β PIX. We quantitate the positive impact of FAK expression on cell spreading and Rac1 activation and targeting. We show that FAK can tyrosine-phosphorylate β PIX and increase its binding to Rac1. FAK-facilitated activation of Rac1 via β PIX may be an important mechanism for the promotion of cell spreading.

MATERIALS AND METHODS

Cell Culture, DNA Constructs, and Transfection

FAK null (FAK⁻) and FAK reexpressing (FAK⁺) mouse embryo fibroblasts were generous gifts from Dr. Steve Hanks, Vanderbilt University (Owen *et al.*, 1999) and were maintained in Dulbecco's modified medium (DMEM; Sigma, St. Louis, MO) that was supplemented with 10% fetal bovine serum (Atlanta Biological, Atlanta, GA), 2 mM L-glutamine (Invitrogen-BRL, Grand Island, NY), penicillin G, streptomycin, and amphotericin B (Invitrogen-BRL). The same medium was used for mouse embryo fibroblasts (MEFs) that were obtained from ATCC (Rockville, MD). Mouse fibroblasts homozygous for the deletion of genes for Src, Yes, and Fyn (SYF) were a generous gift from Phillippe Soriano (Fred Hutchinson Cancer Center, Seattle, WA) and were maintained in the same medium. GFP chimeras of L61Rac1 and N17Rac1 were gifts from Dr. Klaus Hahn (University of North Carolina at Chapel Hill). Flag-tagged β PIX constructs, including the wild-type and a doubly mutated β PIX that neither functions as a GEF nor binds to PAK (β PIX-SH3/DH: W43J, L238R, L239S) were made as described previously (Shin *et al.*, 2004), as was β PIX-GST (ten Klooster *et al.*, 2006). EGFP-FAK was made in the Romer lab as described elsewhere (Cooley *et al.*, 2000). The avian FAK kinase domain (amino acids 411-686) and a kinase dead (K454R) mutant were generated in baculovirus-transfected Hifive insect cells, and were generously provided by Michael Eck, Dana-Farber Cancer Institute (Harvard University, Boston, MA). Myristylated FAK was a gift from Dr. Silvio Gutkind (National Institutes of Health, Bethesda, MD). The dominant negative FAK construct Dter is an 18-kDa truncation mutant of the FAK carboxy-terminus and was a gift from Dr. Mike Schaller (UNC, Chapel Hill, NC; Thomas *et al.*, 1999; Prutzman *et al.*, 2004).

Transient transfections were accomplished using Lipofectamine Plus (Invitrogen-BRL) and standard product protocols. Briefly, cells were plated 24 h before transfection. Cells were washed and then incubated for 3 h in serum-free DMEM medium containing plasmid DNA mixed with Lipofectamine and Plus reagent. The medium was then replaced with DMEM containing 10% FBS and incubated for 48 h before cells were prepared for immunofluorescence or immune replica analysis.

Cell-spreading Assay

Phase-contrast movies were made by plating cells onto fibronectin-coated 35-mm glass bottom microwell dishes (Plastek Cultureware, Ashland, MA). Phase-contrast images were acquired at 1-min intervals up to 50 min after initial plating using a Nikon TE200 microscope (Melville, NY) a Coolsnap HQ CCD camera (Roper, Duluth, GA), and Openlab software (Improvision, Lexington, MA), and converted to QuickTime movie format. Cell spreading rates were determined by measuring cell area as a function of time. Coverslips (no. 1, Warner Instruments, Hamden, CT) were incubated with 25 μ g/ml fibronectin in PBS (Invitrogen-BRL) at 4°C overnight and then assembled into flow chambers (Warner). Cells were plated onto coverslips in standard culture medium and were observed until initial attachment was achieved. Cells were then perfused with standard culture media at a flow rate of ~2 ml/min. For all work with live cells, temperature was maintained at 37°C in the chamber with both an inline fluid heater (Ismatec, Boston, MA) and an objective heater (Biotechs, Eugene, OR). An original MATLAB code (Mathworks, Natick, MA) was used to determine cell area from each phase-contrast image. A Gaussian smoothing filter was applied to each image to remove any sudden intensity changes due to noise. A Laplacian transformation was then applied to the smoothed image to determine points of sudden intensity change, which correlate with the cell edge. The result was a binary image of the cell edge. The area contained within this edge was calculated and converted to units of area (μ m²).

Antibodies

Primary antibodies used in this study include the following: Anti-FAK polyclonal antisera 5158 (made by the Romer lab); anti-Flag polyclonal clone F7425 (Sigma, St. Louis, MO); anti-talin polyclonal rabbit antisera TnC22 (a gift from Dr. Susan Craig, Johns Hopkins University, Baltimore, MD); monoclonal anti-Rac1 clones 23A8 (Upstate, Charlottesville, VA) and 102 (BD Biosciences, San Diego CA); polyclonal AB3829 against β PIX (Chemicon, Temecula, CA); anti-integrin β 1 rat monoclonal clone 9EG7 (BD Biosciences); monoclonal anti-vinculin clone 7F9 (a gift from Dr. Alexey Belkin, Holland Labs, Rockville, MD); polyclonal ab6556 rabbit antisera against GFP (Abcam, Cambridge, MA); rabbit anti-GST polyclonal antibody (Invitrogen), and monoclonal anti-phosphotyrosine clone py20 (BD Biosciences). Affinity cross-adsorbed secondary antibodies including rhodamine-conjugated donkey anti-Rat IgG, Cy3-conjugated goat anti-mouse and goat anti-rabbit IgG, Cy5-conjugated goat anti-mouse and goat anti-rabbit IgG, and FITC-conjugated goat anti-rabbit IgG were purchased from Jackson ImmunoResearch Laboratories (West Grove, PA). FITC-conjugated donkey anti-mouse IgG was purchased from Chemicon (Temecula, CA). Rhodamine-conjugated phalloidin for actin staining was purchased from Molecular Probes (Eugene, OR). Horseradish peroxidase-conjugated anti-mouse and anti-rabbit secondary antibodies were obtained from ICN Biochemicals (Costa Mesa, CA).

Immunofluorescence Staining and Epifluorescence Microscopy

Cells were plated on FN-coated glass coverslips for 2 h. Cells were then permeabilized for 2 min with 0.5% Triton X-100 (Fisher Scientific, Hampton, NH) in 3% paraformaldehyde (Sigma) followed by fixation with 3% paraformaldehyde for 20 min. Antibody incubations were done for 30 min. Cells were observed on an epifluorescence Nikon TE-200 microscope. Images were captured with a Coolsnap HQ camera (Roper) with Openlab software (Improvision).

Analysis of Rac1 Localization at Focal Adhesions

Images of endogenous or ectopically expressed Rac1 or the focal adhesion proteins (vinculin, talin, or β 1 integrin) were acquired with Openlab software as described above. The percentage of focal adhesion areas occupied by Rac1 was determined using an original automation. First, a binary mask corresponding to total focal adhesion area was made from the vinculin or talin or β 1 integrin images, and the total focal adhesion area was calculated. Then, a mask corresponding to regions of Rac1 localization at focal adhesions was made. The ratio of the two binary masks yielded the percentage of focal adhesion area showing Rac1 colocalization. Optimal spectral separation of Rac1 and other focal adhesion protein detection was achieved when possible by using Cy5-conjugated secondary antibody to label vinculin in cells expressing Rac-GFP chimeras and by using FITC-conjugated secondary antibody to label talin for samples in which endogenous Rac1 was identified using Cy5-conjugated antibodies. In cells transfected with β PIX-Flag, FITC-conjugated secondary antibody was used to label Flag and identify transfected cells, whereas Cy3- and Cy5-conjugated secondary antibodies were used to label β 1 integrin and Rac1, respectively.

Rac1 Activity Assay and Western Blotting

The cDNA of the p21-binding domain (PBD) from human PAK1 (amino acids 67-150; generous gift from Dr. Keith Burrridge, University of North Carolina at Chapel Hill) that had been cloned into the bacterial expression vector pGEX-4T3 was expressed in *Escherichia coli* as a glutathione S-transferase (GST) fusion protein. This PBD-GST fusion protein was purified and immobilized on glutathione-Sepharose beads (Benard *et al.*, 1999). Cells were washed with

ice-cold HEPES buffer and then lysed with lysis buffer (50 mM Tris, pH 7.6, 150 mM NaCl, 0.5 mM $MgCl_2$, 1% Triton X-100, 10 μ g/ml leupeptin, 10 μ g/ml aprotinin, 1 mM PMSF, 0.5 mM sodium vanadate). Cell lysates were clarified by centrifugation at $20,000 \times g$ at $4^\circ C$ for 4 min. GST-PBD, 50 μ g, immobilized on glutathione-Sepharose beads was added to $\sim 500 \mu$ g of protein from cell lysates and incubated at $4^\circ C$ with rotation for 60 min. The beads were then washed three times with lysis buffer and boiled in Laemmli sample buffer (Laemmli *et al.*, 1970). GST-PBD bound active Rac1 (in the GTP-bound form) was detected by Western blotting using an mAb against Rac1. Total Rac1 was detected by immunoblotting in samples from corresponding cell lysates. For Western blot analysis, after blocking with 1% BSA in TBST (50 mM Tris-HCl, pH 7.6, 150 mM NaCl, 0.5% Tween 20) overnight, membranes were incubated with appropriate primary antibodies for 1 h at room temperature, washed three times with TBST, and incubated with horseradish peroxidase-conjugated goat anti-mouse or goat anti-rabbit IgG. Proteins were visualized using chemiluminescence (Amersham Biosciences, Piscataway, NJ) and exposure to x-ray film (Eastman Kodak, Rochester, NY). To quantify relative Rac1 activity, a clear image of the autoradiograph was taken using an Epson Perfection scanner (model 2450; Long Beach, CA). The intensity of the bands was then analyzed and normalized to the total cellular Rac protein band using a software-based algorithm in NIH image (version 1.62). Rac1 activity of FAK $-$ cells at 0 min was designated as 100%.

In Vitro FAK Kinase Assay

Full-length murine β PIX cDNA (generous gift of Peter Hordijk, Sanquin Research and Landsteiner Laboratory, University of Amsterdam, The Netherlands) was cloned into the bacterial expression vector pGET-4T3 and expressed in *E. coli* BL21 (Stratagene, La Jolla, CA). The β PIX-GST fusion protein was purified from bacterial lysates, immobilized on glutathione-Sepharose beads, and then released with elution buffer (50 mM Tris-HCl, pH 8.0, 10 mM reduced glutathione; Sigma). Cells were transfected with either full-length FAK or the truncated carboxy-terminus FAK mutant Dter that lacks the kinase domain. Both FAK constructs were EGFP-tagged. 48 h after transfection protein lysates were obtained using modified RIPA buffer (0.1% DOC, 0.1% Triton X-100, 2 mM EDTA, 1 mM PMSF, 2 mM sodium vanadate, 20 μ g/ml leupeptin, 20 μ g/ml aprotinin in PBS). EGFP-FAK or EGFP-Dter were immunoprecipitated with anti-GFP antibody from 500 μ g of protein lysates for 2 h and captured on protein A-Sepharose by rotation for 1 h at $4^\circ C$. After four washes in lysis buffer EGFP-FAK or EGFP-Dter immunoprecipitates were resuspended in kinase buffer (50 mM Tris, pH 7.4, 5 mM $MnCl_2$, and 5 mM $MgCl_2$). Approximately 2 μ g of purified β PIX-GST and 20 μ M of ATP (final concentration) were added to the beads as substrate to a total volume of 60 μ l and incubated at $37^\circ C$ for 30 min on a shaker to keep the beads in suspension. In other experiments, aliquots of GST-wtFAK411-686 or GST-FAK411-686K454R (1, 3, or 6 μ g) were added to 2 μ g of purified GST- β PIX or 4 μ g of purified GST in kinase buffer with or without 20 μ M of ATP (final concentration) in a total volume of 60 μ l and incubated at $37^\circ C$ for 30 min. The kinase reactions were stopped by the addition of sample buffer and analyzed using SDS-PAGE, transfer to nitrocellulose, and serial immunoblotting with antibodies against GFP (or GST), β PIX, and phosphotyrosine. Some experiments were done in the presence of the Src inhibitor PP2 (10 μ M; EMD Biosciences, San Diego, CA).

In Vitro Binding Assay for β PIX and Rac1

FAK $-$ cells were cotransfected with β PIX-Flag and either EGFP-Dter, EGFP-FAK, or myristylated FAK. Two days after transfection, cells were washed with ice-cold HEPES buffer and then lysed with modified RIPA buffer. Cell lysates were clarified by centrifugation at $\sim 20,000 \times g$ at $4^\circ C$ for 4 min. Lysate volumes were then normalized for equal protein content using the bicinchoninic assay (Pierce, Rockford, IL). To immunoprecipitate β PIX-Flag, lysates containing 500 μ g of protein were equalized for volume with lysis buffer and incubated at $4^\circ C$ with rotation first with anti-Flag antibody and then with protein A-Sepharose beads (Jackson). The beads with the bound, immunoprecipitated β PIX-Flag were then washed four times with lysis buffer before adding 5 μ g of purified GST-Rac1 (gift of Ian Macara, University of Virginia at Charlottesville). These mixtures were then incubated for 3 h or overnight at $4^\circ C$ with rotation. Beads were then washed again with lysis buffer. Proteins were released from the beads by boiling in Laemmli sample buffer and subjected to SDS-PAGE using 4–15% gradient polyacrylamide gels. Proteins were then transferred to nitrocellulose membranes for Western blotting (Towbin *et al.*, 1979). The membranes were probed serially using primary antibodies against Rac1, phosphotyrosine, and the Flag epitope tag. Each of these was followed by the appropriate horseradish peroxidase-conjugated anti-mouse or anti-rabbit IgG secondary antibody. Processing for chemiluminescence was as detailed above. Before reprobing with different antibodies, membranes were immersed in stripping buffer (2% SDS, 0.6% β -mercaptoethanol, 62.5 mM Tris-Cl, pH 6.8) at $60^\circ C$ for 30 min with frequent shaking, and washed thoroughly with TBST.

Statistical Analysis

The Student's *t* test was used to analyze Rac1 activation assay data and the effects of altered β PIX expression on cell surface area. The Mann-Whitney

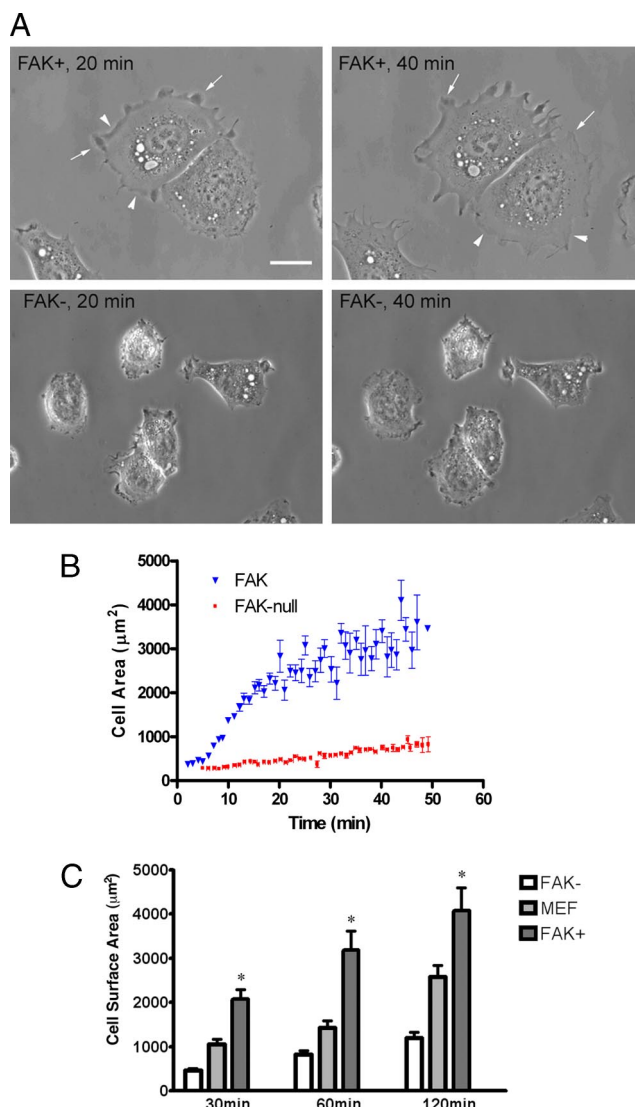


Figure 1. FAK null cells spread poorly on fibronectin. (A) FAK+ and FAK $-$ fibroblasts were plated onto fibronectin-coated dishes. Phase-contrast images acquired at 20 and 40 min are shown. FAK+ cells (top panels) rapidly established broad lamellipodia as indicated by the arrows and membrane ruffles (arrowheads). Both of these features failed to develop well in FAK $-$ cells (bottom panels). Scale bar, 10 μ m. (B) Cell spreading rates were determined by measuring surface area as a function of time for both FAK+ (\blacktriangledown , $n = 11$) and FAK $-$ cells (\blacksquare , $n = 9$) by phase-contrast microscopy. After initial attachment (~ 5 – 7 min), cells were perfused with media at ~ 2 ml/min. Images were collected at 1-min intervals up to 50 min. Mean surface area data (\pm SE) are shown for each time point. Compared with their FAK $-$ counterparts, FAK+ cells spread at nearly twice the rate to a maximum area more than three times as large. (C) FAK $-$, MEF, and FAK+ fibroblasts were plated onto fibronectin-coated coverslips for 30, 60, or 120 min. Images of cells labeled with rhodamine-conjugated phalloidin were used for cell size quantification with Openlab software. Cell surface area units are μm^2 . FAK+ fibroblasts were larger than FAK $-$ cells at each time point indicated by an asterisk ($*p < 0.001$).

test was used to evaluate maximum area (A_{max}) and time to 50% of maximum area (t_{50}) data for cell spreading from individual curve fit analyses, and data on Rac1 localization to focal adhesions. *p* values are supplied in each figure legend, and significance was adjudged to be present at $p < 0.05$ for all data. All graphs include SE bars.

RESULTS

Quantitative Analysis of Limited Spreading in FAK Null Cells

FAK⁻ and FAK⁺ cells were trypsinized and then plated onto FN-coated 35-mm microwell dishes with glass bottoms. Phase-contrast images were acquired at 1-min intervals up to 50 min after initial adhesion. Cell surface areas were then quantified as described in *Materials and Methods*. Supplementary QuickTime movie files S1 and S2 are submitted for complete time-lapse data on FAK⁻ and FAK⁺ cells, respectively. FAK⁺ cells spread well and developed many lamellipodia and filopodia within 20 min of plating on FN, continued active membrane extension throughout, and were larger than FAK⁻ cells (Figure 1, A and B). The smaller FAK⁻ cells had restricted membrane ruffles and minimal lamellipodial development. Nuclear size was also smaller in the FAK⁻ cells and averaged 80% of the surface area of nuclei in FAK⁺ cells. Quantitative analysis of spreading rates and areas were determined by measuring surface area as a function of time for 11 FAK-reexpressing cells and 9 FAK-null cells (Figure 1B). The mean and SEs for measurements on each cell type at each time point are shown in the figure and listed below. One-phase exponential association curves were fit to data from each cell (not shown in figure), and values for the maximum area (A_{\max}) and time to 50% of maximum area (t_{50}) were calculated for the family of curves generated by each cell type separately. R^2 values for the

curves used for the cell spreading analyses for data shown in Figure 1B were 0.9450 ± 0.01066 for FAK⁺ cells and 0.9106 ± 0.02049 for FAK⁻ cells. Results indicate that FAK reexpressing cells have a larger maximum area ($A_{\max, \text{FAK}} = 3577.0 \pm 607.2 \mu\text{m}^2$, vs. $A_{\max, \text{FAK-null}} = 1122.0 \pm 202.0 \mu\text{m}^2$, $p = 0.0017$) and spread faster ($t_{50, \text{FAK}} = 13.11 \pm 1.63 \text{ min}$, vs. $t_{50, \text{FAK-null}} = 23.92 \pm 4.75 \text{ min}$, $p = 0.05$). Additionally, the spreading performance of FAK⁻ and FAK⁺ cells was analyzed in parallel with that of control MEF cells (Figure 1C). Surface area data were calculated from images of paraformaldehyde-fixed cells of each type using an algorithm in Openlab software after labeling with rhodamine-conjugated phalloidin. FAK⁻ cells did not spread as well as FAK⁺ cells at all time points ($p < 0.001$ at 30, 60, and 120 min), and values for MEF cells were in between the other two populations at each interval.

FAK Augmentation of Adhesion-induced Rac1 Activation

Rac1 activity was analyzed in lysates of FAK⁻ and FAK⁺ cells before (time 0 = suspension) and after attachment to fibronectin-coated Petri dishes for 30, 60, and 120 min. Rac1 was activated by adhesion to fibronectin in both FAK⁻ and FAK⁺ cells as measured by a GST affinity pulldown assay using the Rac-binding domain of PAK1 (Figure 2A). Cell lysates (15 μg) from each sample were blotted with anti-Rac1 antibody for total Rac1 as a loading control, and this demonstrated an equal amount of total Rac1 in the two cell

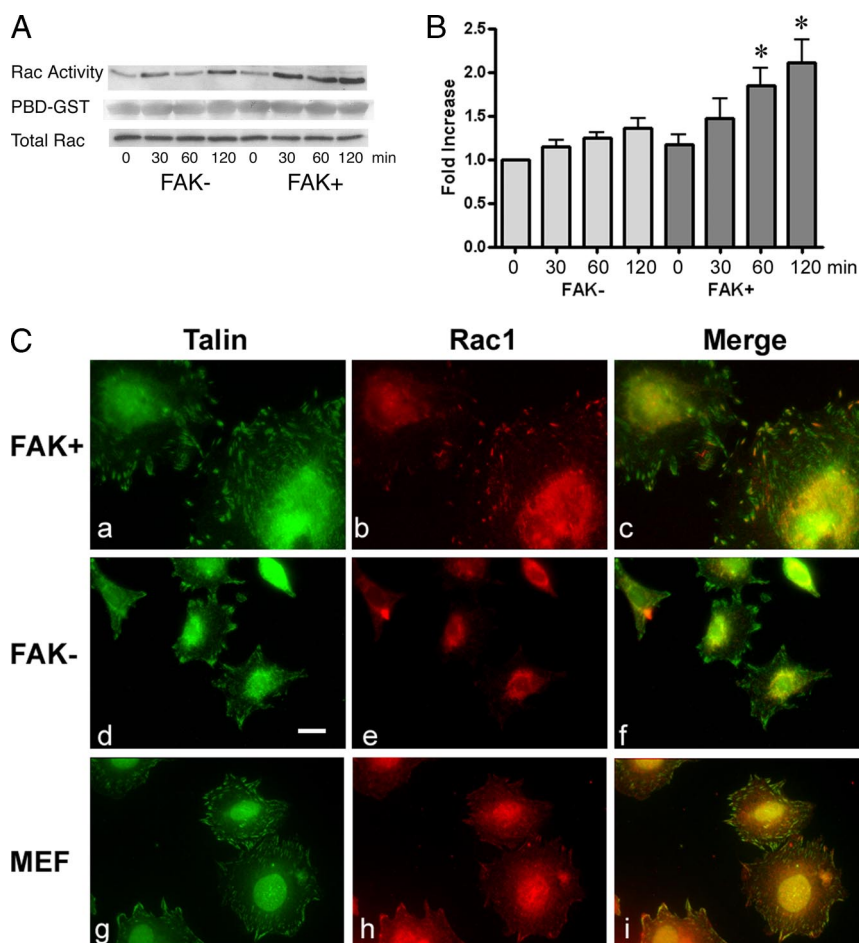


Figure 2. FAK increased Rac1 activation and translocation to focal adhesions. (A) FAK⁻ and FAK⁺ (left and right 4 lanes, respectively) fibroblasts were plated on fibronectin-coated dishes for the times indicated (0 min = suspension). A PBD-GST affinity pulldown Rac1 activity assay was done on 500 μg of protein from each lysate (top row). Coomassie blue staining of the membrane verified the addition of an equal amount of PBD-GST substrate to each sample (middle row). Western blotting of separate portions of each whole-cell lysate showed equal amounts of total Rac1 from each cell type at all studied time points (bottom row). Rac activation was more prominent in FAK⁺ cells. (B) Three sets of Rac activity assay results were used for densitometry and statistical analysis of the differences in adhesion-induced Rac1 activation between FAK⁻ and FAK⁺ cells (left and right 4 bars, respectively). Blots were scanned using an Epson scanner (model 2450) and the intensity of each of the active Rac1 bands pulled down by the PBD-GST was normalized to the total cellular Rac protein band and calculated by a software-based algorithm using NIH image software (version 1.62). Rac1 activity of FAK⁻ cells at 0 min was assigned the value of 100%, and relative values are shown for the other samples. SE bars are shown. Asterisks indicate a significant increase in Rac1 activity in FAK⁺ cells compared with FAK⁻ cells at the same time point ($p < 0.05$). (C) FAK⁺ (a–c), FAK⁻ (d–f), and MEF (g–i) cells were plated on FN-coated coverslips for 2 h before fixation and preparation for immunofluorescence analysis. Talin is shown in green (FITC channel data; a, d, and g), and Rac1 is shown in red (Cy5 channel data; b, e, and h). Colocalization appears yellow-orange in the merged images shown in c, f, and i. Rac1 was seen in focal adhesions in FAK⁺ cells and MEF more often than in FAK⁻ cells. Scale bar, 10 μm .

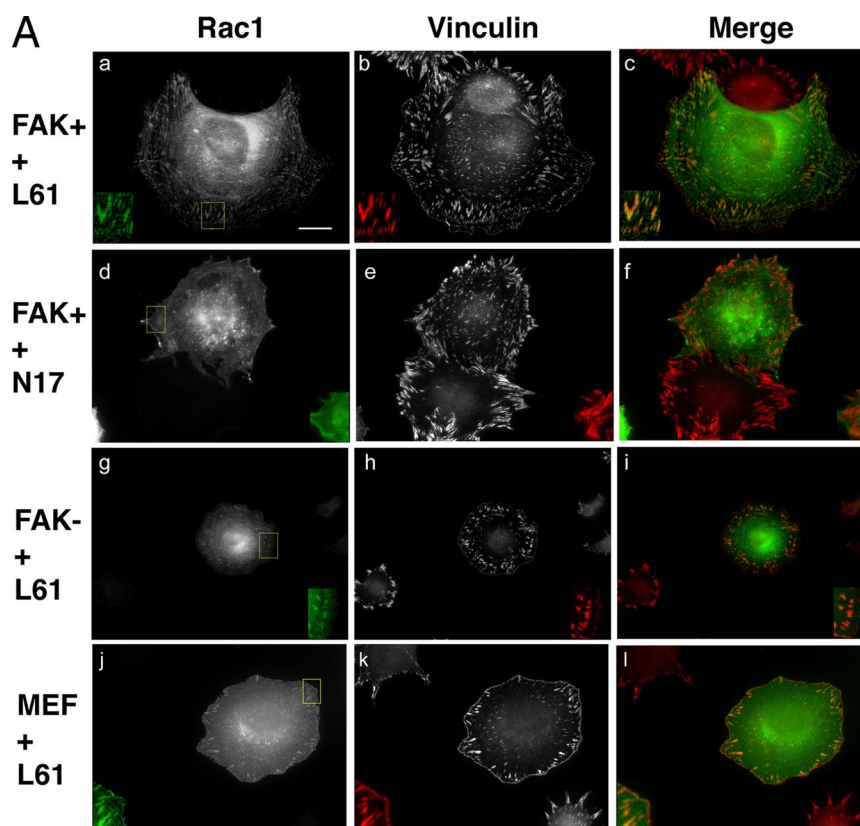


Figure 3. Rac1 activity and focal adhesion targeting: (A) FAK+ (a–c), FAK– (g–i), and MEF (j–l) cells were transfected with GFP-tagged L61Rac1. FAK+ cells were transfected with GFP-tagged L61Rac1 (dominant negative, d–f). Two days later cells were plated onto fibronectin-coated coverslips for 2 h and prepared for immunofluorescence studies. GFP-Rac1 signal (a, d, g, and j) and vinculin antibody labeling (b, e, h, and k; Cy5 channel data) are shown. GFP-Rac is shown in green, vinculin is shown in red, and colocalization appears yellow-orange in the merged images in panels c, f, i, and l. The boxed areas in a, d, g, and j were magnified (2 \times) and are shown in individual insets for each panel. Scale bar, 10 μ m. (B) An automated image analysis routine (see *Materials and Methods*) was used to measure the percentage of focal adhesion surface area occupied by endogenous Rac1 in non-transfected FAK– and FAK+ cells (pair of bars at left, n = 22 FAK– and 22 FAK+), and by the ectopically expressed L61Rac1 (middle pair of bars, n = 10 FAK– and 6 FAK+), or N17Rac1 (pair of bars at right, n = 6 FAK– and 5 FAK+). Bars are SEs. Asterisks indicate statistically significant differences from cell type-matched nontransfected controls ($p < 0.01$ in all cases, details in text).

populations at all studied time points. These data show that activation of Rac1 began minutes after plating and increased through 2 h. FAK+ cells exhibited higher Rac1 activity compared with FAK– cells at each time point tested and also showed a more robust rise in response to integrin-mediated adhesion (Figure 2A). Statistical analysis of densitometry data from three of these experiments is shown in Figure 2B. We normalized Rac1 activity using the Rac1 activity of FAK– cells at 0 min (in suspension) as 100%. Significant increases in Rac1 activity were seen in the FAK+ cells at 60 min ($p < 0.05$) and 120 min ($p < 0.01$) after plating on fibronectin as compared with the FAK– population. These results indicated that FAK facilitates Rac1 activation during integrin-mediated cell adhesion.

Increased Rac1 Localization to Focal Adhesions in FAK+ Cells

To further investigate the molecular basis of differences in cell spreading between FAK+ and FAK– cells, we studied

the subcellular distribution of Rac1. After 2 h of adhesion to fibronectin-coated glass coverslips, FAK+ cells showed many well-established focal complexes, focal adhesions, and fibrillar adhesions, as demonstrated by the talin labeling shown in Figure 2C. Surprisingly, anti-Rac1 antibody staining revealed the translocation of Rac1 to many peripheral focal adhesions in FAK+ cells (Figure 2C, b and c). Rac1 labeling was not completely congruent with talin staining, but was restricted to a subset of the focal adhesion area toward the cell perimeter. This focal adhesion translocation was verified with two different monoclonal antibodies (displayed data are from experiments using BD Biosciences' clone 102; data from studies with Upstate's clone 23A8 are not shown) was verified in control MEF cells (h and i) and was seen much less in FAK– cells (e and f). Rac1 focal adhesion localization was analyzed quantitatively and expressed as the percentage of focal adhesion surface area (\pm SE) that was occupied by Rac1, as shown in Figure 3B

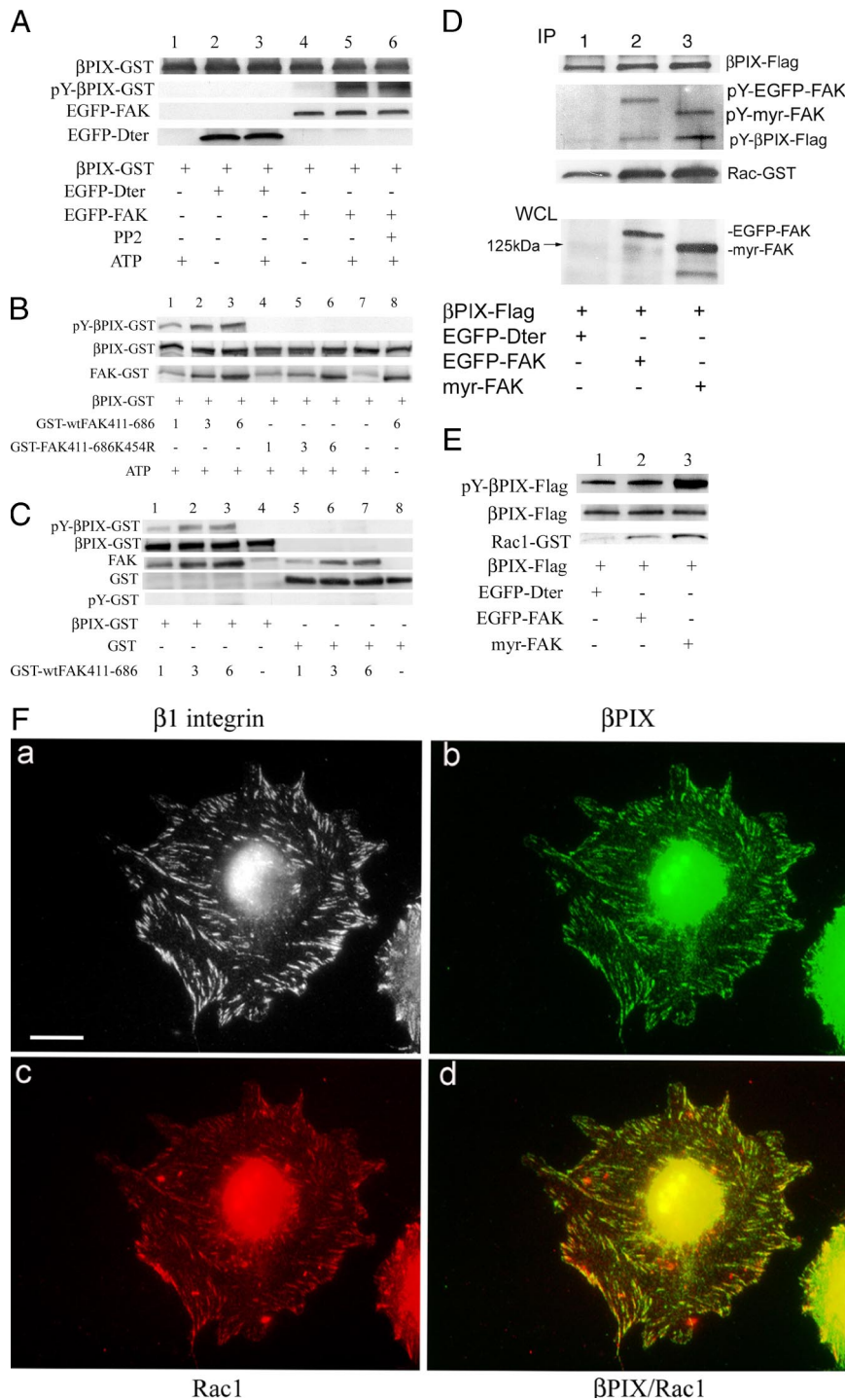
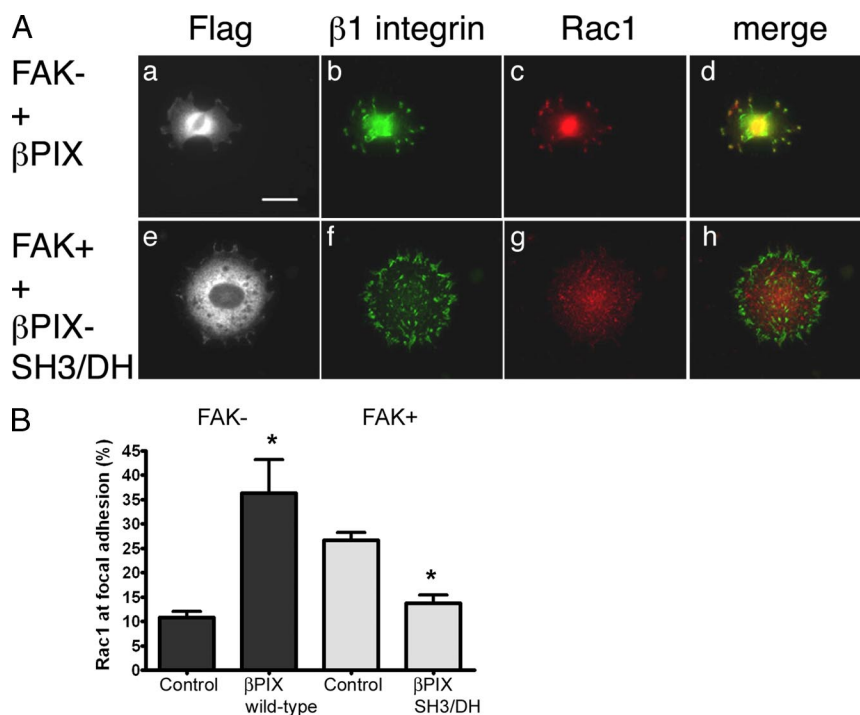


Figure 4. FAK association with βPIX and FAK-mediated tyrosine-phosphorylation of βPIX. (A) FAK⁻ cells were transfected with EGFP-tagged wild-type FAK (lanes 4–6), the FAK mutant Dter that lacks a kinase domain (lanes 2–3), or nothing (lane 1). EGFP-Dter and EGFP-FAK were immunoprecipitated using anti-GFP antibody and protein A-Sepharose. About 2 μg of purified βPIX-GST was then added to each sample containing mock, EGFP-Dter, or EGFP-FAK immunoprecipitates for an in vitro kinase assay in the presence of 20 μM ATP (omitted in lanes 2 and 4). The kinase reaction mixture was analyzed by SDS-PAGE and serial immunoblotting with anti-GFP, anti-βPIX, and pY20 antibodies. FAK-mediated tyrosine phosphorylation of βPIX is shown. Lane 6 shows no change in the tyrosine phosphorylation of βPIX by FAK in the presence of the Src inhibitor PP2 (10 μM). (B) Purified FAK tyrosine-phosphorylates βPIX-GST in vitro. Purified βPIX-GST, 2 μg, was incubated with 1, 3, or 6 μg of purified GST-tagged wild-type FAK (GST-wtFAK411-686; lanes 1–3, respectively, and 6 μg in lane 8) or kinase dead FAK mutant (GST-FAK411-686K454R; lanes 4–6) in kinase buffer for 30 min at 37°C in the presence of 20 μM ATP (omitted in lane 8). The kinase reaction mixture was analyzed by SDS-PAGE and immunoblotting with anti-GST and pY20 antibodies. No FAK was used in lane 7. Wild-type FAK kinase domain, but not the kinase dead FAK mutant, tyrosine-phosphorylates βPIX-GST in a dose-dependent manner. (C) FAK specifically tyrosine-phosphorylates βPIX. Purified βPIX-GST (2 μg, lanes 1–4) or 4 μg of purified GST (lanes 5–8) were incubated with 1, 3, 6, or 0 μg of purified GST-wtFAK411-686 (lanes 1 and 5, 2 and 6, 3 and 7, and 4 and 8, respectively) in kinase buffer for 30 min at 37°C in the presence of 20 μM ATP. The kinase reaction mixture was analyzed by SDS-PAGE and immunoblotting with anti-GST and pY20 antibodies. Wild-type FAK tyrosine-phosphorylates βPIX-GST but not the GST alone in a dose-dependent manner. (D) FAK null cells were cotransfected with Flag-tagged wild-type βPIX and either EGFP-Dter (lanes labeled 1), EGFP-FAK (lanes labeled 2), or myristylated-FAK (lanes labeled 3). Two days later, βPIX-Flag was immunoprecipitated using anti-Flag antibody from lysates of each cell population that had been normalized for total protein. βPIX-Flag immunoprecipitates were then incubated with purified recombinant Rac1-GST. These samples were then processed by SDS-PAGE, transferred to nitrocellulose, and Western-blotted with an anti-phosphotyrosine antibody (rows 2–4). Then, the membrane was stripped and re-probed with anti-Rac1 antibody (top row). At the bottom of the figure, whole-cell lysates (WCL) from cells transfected as detailed beneath the figure were immunoblotted with an anti-FAK antibody. (E) SYF cells were cotransfected with Flag-tagged wild-type βPIX and either EGFP-Dter (lanes labeled 1), EGFP-FAK (lanes labeled 2), or myristylated-FAK (lanes labeled 3). This experiment was similar in design to the FAK⁻ cell experiment in D. βPIX-Flag was immunoprecipitated using anti-Flag antibody from lysates of each cell population and βPIX-Flag immunoprecipitates were then incubated with purified recombinant Rac1-GST. These samples were then processed by SDS-PAGE, transferred to nitrocellulose, and immunoblotted with an anti-phosphotyrosine antibody (row 1). Then, the membrane was stripped and re-probed with anti-Rac1 antibody (third row). Finally, the immunoprecipitates were immunoblotted for βPIX-Flag (middle row). (F) FAK⁺ cells (without transfection) were plated onto fibronectin-coated coverslips for 2 h and prepared for immunofluorescence analysis of β1 integrin (a), βPIX (b), and Rac1 (c) localization using antibodies raised in rat, rabbit, and mouse, respectively. Affinity cross-adsorbed secondary antibodies were used to label these three targets as follows: β1 integrin with rhodamine (shown in gray scale), βPIX with Cy5 (shown in green), and Rac1 with FITC (shown in red). Panel d is a merge of the βPIX and Rac1 images, and colocalization appears yellow-orange. Scale bar, 10 μm.

probed with anti-Rac1 antibody (bottom row). Finally, the immunoprecipitates were immunoblotted for βPIX-Flag (top row). At the bottom of the figure, whole-cell lysates (WCL) from cells transfected as detailed beneath the figure were immunoblotted with an anti-FAK antibody. (E) SYF cells were cotransfected with Flag-tagged wild-type βPIX and either EGFP-Dter (lanes labeled 1), EGFP-FAK (lanes labeled 2), or myristylated-FAK (lanes labeled 3). This experiment was similar in design to the FAK⁻ cell experiment in D. βPIX-Flag was immunoprecipitated using anti-Flag antibody from lysates of each cell population and βPIX-Flag immunoprecipitates were then incubated with purified recombinant Rac1-GST. These samples were then processed by SDS-PAGE, transferred to nitrocellulose, and immunoblotted with an anti-phosphotyrosine antibody (row 1). Then, the membrane was stripped and re-probed with anti-Rac1 antibody (third row). Finally, the immunoprecipitates were immunoblotted for βPIX-Flag (middle row). (F) FAK⁺ cells (without transfection) were plated onto fibronectin-coated coverslips for 2 h and prepared for immunofluorescence analysis of β1 integrin (a), βPIX (b), and Rac1 (c) localization using antibodies raised in rat, rabbit, and mouse, respectively. Affinity cross-adsorbed secondary antibodies were used to label these three targets as follows: β1 integrin with rhodamine (shown in gray scale), βPIX with Cy5 (shown in green), and Rac1 with FITC (shown in red). Panel d is a merge of the βPIX and Rac1 images, and colocalization appears yellow-orange. Scale bar, 10 μm.

Figure 5. β PIX and Rac1 targeting. (A) FAK⁻ cells that were transfected with Flag-tagged wild-type β PIX (top row) and FAK⁺ cells that were transfected with Flag-tagged double mutant β PIX-SH3/DH (bottom row) were plated on fibronectin-coated glass 48 h after transfection. After 2 h, samples were fixed and labeled with rabbit anti-Flag (a and e), rat anti- β 1 integrin (b and f), and mouse anti-Rac1 (c and g) antibodies. Merged images of β 1 integrin and Rac1 data are shown at the right (d and h). Scale bar, 10 μ m. (B) The percentage of the total focal adhesion area per cell that was occupied by endogenous Rac1 was determined by the Openlab automation detailed in *Materials and Methods*. Total focal adhesion surface area was derived from β 1 integrin staining. Wild-type β PIX expression tripled Rac1 focal adhesion targeting in FAK⁻ cells (n = 22 controls and 5 transfected cells). In FAK⁺ cells, β PIX-SH3/DH expression halved Rac1 translocation to focal adhesions. Data shown are means \pm SEs. (n = 37 controls and 15 transfected cells). *p < 0.01.



(pair of bars on left). The percentage of the peripheral focal adhesion surface area defined by talin staining that was occupied by Rac1 averaged $28.9 \pm 2.9\%$ in FAK⁺ cells and only $8.8 \pm 1.2\%$ in FAK⁻ cells ($p < 0.0001$).

Activated Rac1 Localization to Focal Adhesions

To study the relationship between the activity of Rac1 and its subcellular localization, we investigated focal adhesion targeting of constitutively active (L61) and dominant negative (N17) Rac1 (Figure 3, A and B). L61Rac1-GFP prominently colocalized with vinculin at focal adhesions in FAK⁺ cells and occupied nearly the entire surface area of each focal adhesion (Figure 3A, a–c). This same pattern of focal adhesion targeting was demonstrated by L61Rac1-GFP in MEF cells (Figure 3A, j–l). In marked contrast, very little Rac1-GFP targeting to focal adhesions was found in FAK⁺ cells that had been transfected with the dominant negative N17Rac1-GFP, (Figure 3A, d–f). Notably, L61Rac1-GFP showed robust focal adhesion localization in FAK⁻ cells, indicating that the recruitment of Rac1 to focal adhesions may be determined by the level of Rac1 activity (g–i). Quantitative evaluation (mean values and SEs) of Rac1 targeting in FAK⁻ and FAK⁺ cells is displayed in Figure 3B. The changes associated with expression of the constitutively active or dominant negative forms are shown. Rac61L-GFP showed increased focal adhesion localization over endogenous Rac1 in FAK⁺ cells ($p = 0.0006$) and in FAK⁻ cells ($p = 0.0009$). Further, we noted that L61Rac1-GFP improved cell spreading and lamellipodial extension in the FAK⁻ cells (see Figure 6A). N17Rac1-GFP showed decreased targeting to focal adhesions compared with endogenous Rac1 in both cell types ($p = 0.0025$ for FAK⁺ and $p < 0.0001$ for FAK⁻). Additional investigation showed that the expression of exogenous wild-type Rac1-GFP did not affect the focal adhesion targeting of Rac1. These data suggest that the GTP-bound or active form of Rac1 is preferentially targeted to focal adhesions and can change cell spreading behavior (see also Figure 6A).

FAK-mediated Tyrosine Phosphorylation of β PIX

To identify the mechanisms underlying FAK facilitation of both Rac1 activation and Rac1 targeting to focal adhesions, we studied interaction between Rac1-associated GEFs and FAK. To begin, nitrocellulose membranes used for Rac activity assays were reprobbed with anti-phosphotyrosine antibody. Interestingly, β PIX was the only protein that was tyrosine-phosphorylated and pulled down with Rac1 by PBD in the Rac1 activity assays.

In vitro kinase assays were done to ascertain whether FAK could directly tyrosine phosphorylate β PIX (Figure 4A). FAK⁻ cells were transfected with EGFP-tagged wild-type FAK or the carboxy-terminus truncation mutant of FAK Dter, which lacks a kinase domain. EGFP-Dter and EGFP-FAK were immunoprecipitated using anti-GFP antibody and protein A-Sepharose. Purified β PIX-GST, 2 μ g, that had been produced in *E. coli* was then added to the EGFP-Dter or EGFP-FAK immunoprecipitates together with ATP. These data demonstrated that β PIX was tyrosine-phosphorylated by EGFP-FAK in the presence of ATP, but not by EGFP-Dter. The addition of 10 μ M PP2, a Src inhibitor (lane 6), did not change the tyrosine phosphorylation of β PIX by immunoprecipitated FAK. To be certain that the data observed in these in vitro kinase experiments were due to direct tyrosine phosphorylation of β PIX by FAK, additional in vitro kinase experiments were performed using purified, baculovirus-derived FAK kinase domain (Figure 4, B and C). β PIX, but not GST alone, was tyrosine-phosphorylated by FAK. β PIX was not tyrosine-phosphorylated by kinase-dead (K454R) FAK (Figure 4B, lanes 4–6), or in the absence of ATP (Figure 4B, lane 8). These experiments demonstrated the direct, specific, dose-dependent tyrosine phosphorylation of β PIX by FAK.

To determine whether FAK associates directly with β PIX, we prepared three populations of FAK⁻ cells that expressed β PIX-Flag together with cotransfected EGFP-Dter (48 kDa; Figure 4D, lanes marked 1), EGFP-FAK (155 kDa; lanes

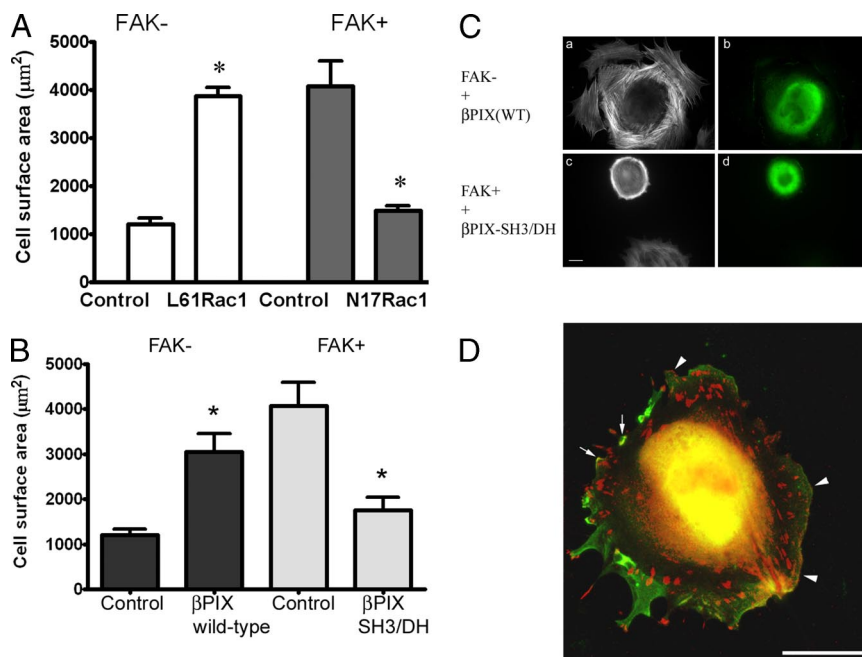


Figure 6. β PIX and cell spreading. (A) Cell surface area was quantified from phalloidin-labeled cell images using Openlab software in FAK⁻ cells transfected with GFP-tagged constitutively active Rac1 (L61) and in FAK⁺ cells transfected with GFP-tagged dominant negative Rac1 (N17). Fixation and labeling were done after 2 d in culture, and cells were plated on fibronectin for 2 h before study. GFP signal was used to identify transfected cells. Constitutively active Rac1 (L61) expression was associated with an increase in mean surface area to three times that of untreated FAK⁻ cells (n = 25 control cells and 8 transfected cells). Dominant negative Rac1 (N17) expression caused a 64% reduction in mean spread cell area in FAK⁺ cells (n = 9 control cells and 8 transfected cells). Data shown are means \pm SEs. *p < 0.001. (B) Cell surface area was quantified from phalloidin-labeled cell images using Openlab software in FAK⁻ cells transfected with wild-type β PIX-Flag and in FAK⁺ cells transfected with β PIX-SH3/DH-Flag. Fixation and labeling were done after 2 d in culture, and cells were plated on fibronectin for 2 h before study. Anti-Flag antibody staining was used to identify transfected cells. Wild-type β PIX expression was associated with a

twofold increase in mean surface area in FAK⁻ cells (n = 21 control cells and 9 transfected cells). β PIX-SH3/DH-Flag caused a 50% reduction in mean spread cell area in FAK⁺ cells (n = 9 control cells and 14 transfected cells). Data shown are means \pm SEs. *p < 0.01. (C) FAK⁻ cells transfected with Flag-tagged wild-type β PIX (top row), and FAK⁺ cells transfected with Flag-tagged double mutant β PIX-SH3/DH (bottom row), were plated on fibronectin-coated glass 48 h after transfection. After 2 h, samples were fixed and labeled for immunofluorescence. Rhodamine phalloidin-labeled images show F-actin (a and c), and anti-Flag antibody labeling shows the transfected cells (b and d). Scale bar, 10 μ m. (D) Wild-type β PIX-Flag (anti-Flag antibody and FITC labeling, shown in green) and vinculin (Cy5 labeling, shown in red) are shown in a transfected FAK⁻ cell. Colocalization appears yellow-orange and is seen in focal adhesions (arrows) and in clusters of focal complexes in membrane ruffles (arrowheads). Scale bar, 10 μ m.

marked 2), or constitutively active (membrane-targeted) myristylated FAK (myr-FAK, 125 kDa; lanes marked 3), respectively. An anti-FAK immunoblot of whole cell lysates (WCL lanes) was done to adjust transfection efficiency. β PIX-Flag was immunoprecipitated with anti-Flag antibody from lysates of each of the three doubly transfected cell populations that had been normalized for total protein and serially immunoblotted with anti-Flag (top row), and anti-phosphotyrosine (rows 2–4) antibodies. We noted that FAK coimmunoprecipitated with β PIX as evidenced by both anti-phosphotyrosine (second set of blots) and anti-FAK (not shown) immunoblotting. In findings that confirmed our *in vitro* kinase assays, anti-phosphotyrosine immunoblotting also revealed that the low baseline levels of phosphotyrosine on β PIX seen in the FAK⁻ cells was increased in the presence of wild-type FAK expression (EGFP-FAK) and was further augmented in the presence of myristylated FAK (“IP lanes,” bottom of the second blot, Figure 4D). To verify that the tyrosine phosphorylation of β PIX observed here was not mediated by Src that might have associated with the FAK immunoprecipitates, this experiment was repeated in SYF cells (Figure 4E) with the same results.

To define the impact of FAK-mediated tyrosine phosphorylation of β PIX on β PIX interaction with Rac1, purified Rac1-GST was added to the immobilized purified β PIX-Flag after the immunoprecipitations described above. The effect of tyrosine phosphorylation on the β PIX-Rac1 interaction was studied by reprobating these immobilized β PIX immunoprecipitates with an anti-Rac1 antibody (IP lanes, third blot, Figure 4D). These data showed that tyrosine-phosphorylated β PIX bound Rac1-GST more effectively than non-tyrosine-phosphorylated β PIX. β PIX loading was comparable in all three lanes (IP lanes, top row, Figure 4D).

Subcellular Localization of β PIX in FAK⁺ Fibroblasts

Because our experimental evidence indicated that β PIX might have mediated the patterns of Rac1 activation and targeting seen in the FAK⁺ cells, we interrogated these cells by immunofluorescence labeling of β 1 integrin in FAK⁺ cells to discern the subcellular localization of endogenous β PIX (Figure 4F). Although β PIX was not often found in focal adhesions, some cells revealed a pattern of antibody staining for endogenous β PIX that corresponded with a portion of cell-matrix adhesions. In these cells β PIX was found in peripheral adhesions. Further, in cells that exhibited β PIX in focal adhesions, the subset of focal adhesion surface area targeted by Rac1 (panel c) reproducibly colocalized with β PIX (panel d). These findings suggested that β PIX interaction with Rac1 may occur in focal adhesions (as has been proposed by ten Klooster *et al.*, 2006).

β PIX Effects on Rac1 Targeting to Focal Adhesions

To further explore the role of β PIX in Rac1 targeting to focal adhesions, FAK⁻ cells were transfected with wild-type β PIX-Flag. Cells were triple-labeled for Rac1, β 1 integrin, and Flag. Expression of ectopic wild-type β PIX rescued Rac1 targeting to focal adhesions in FAK⁻ cells (Figures 5, A and B). Thus, increased β PIX expression recovered Rac1 targeting in FAK⁻ cells (p = 0.0007).

In parallel experiments, FAK⁺ cells were transfected with the double mutant, β PIX-SH3/DH-Flag (W43J, L238R, L239S) with absent GEF activity and absent PAK binding. Expression of this double mutant GEF-negative β PIX decisively hampered Rac1 translocation to focal adhesions in FAK⁺ cells, causing a drop in Rac1 incorporation into focal adhesions (p < 0.0001). These data further implicate β PIX as a specific molecular mediator of Rac1 trafficking by FAK.

Cell Spreading Responses to Changes in Rac1 and β PIX Expression

The effects of Rac1 activation mutants were examined in FAK⁻ and FAK⁺ cells (Figure 6A). Cells were prepared for immunofluorescence study on the second day after transfection, and 2 h after plating on fibronectin-coated coverslips. FAK⁻ cells that were transfected with constitutively active L61-Rac1 had a mean surface area threefold greater than nontransfected controls ($p < 0.0001$). Conversely, FAK⁺ cells transfected with dominant negative N17-Rac1 had 35% the mean surface area of untransfected controls ($p < 0.001$). Thus, Rac1 had a profound effect on cell spreading behavior both in the presence and the absence of FAK expression.

The extent to which β PIX might alter Rac1-mediated cell spreading was then examined. On the second day after transfection, cells were prepared for immunofluorescence analysis 2 h after plating on fibronectin. Increased wild-type β PIX-Flag expression in FAK⁻ cells more than doubled cell size ($p = 0.0007$; Figure 6B). Ectopic β PIX expression also caused morphological modifications in the actin cytoskeleton (Figure 6C). Thus, FAK⁻ cells expressing wild-type β PIX had an active leading edge with many membrane extensions and subcortical actin arrays that were perpendicular to the cell perimeter (Figure 6Ca), features that are not characteristic of untransfected FAK⁻ cells.

FAK⁺ cells transfected with β PIX-SH3/DH-Flag showed decreased spreading ($p = 0.0019$; Figure 6B). FAK⁺ cells transfected with β PIX-SH3/DH-Flag exhibited a smooth leading edge, a rounded morphology, and few membrane extensions (Figure 6C). Changes in the availability and functionality of β PIX were therefore associated with dramatic differences in cell spreading efficiency.

Immunofluorescence analysis of transfected FAK⁻ cells demonstrated that the exogenous Flag-tagged wild-type β PIX colocalized with vinculin in some peripheral focal adhesions, focal complexes, and membrane ruffles and was associated with morphological features seen in rapidly spreading cells including an active ruffling membrane edge (Figure 6D).

DISCUSSION

The work presented here defines a new cellular signaling pathway that actively drives cell spreading in the setting of FAK expression. This pathway may complement the release of circumferential cytoskeletal tension through FAK-mediated inhibition of RhoA (Ren *et al.*, 1999, 2000; Chen *et al.*, 2002; Holinstat *et al.*, 2006) and accelerate lamellipodial extension by adding a second small GTPase-regulated mechanism—the activation of Rac1. The quantitative characterization of cell spreading that is presented here affords some clues to the relative importance of Rho inhibition and Rac activation in the improved spreading efficiency seen in FAK-expressing fibroblasts. Taken together, data shown in Figures 1B and 6A indicate that Rac activation via FAK and β PIX may account for approximately two thirds of the differences in cell spreading between the FAK⁻ and FAK⁺ populations in this study. Our work demonstrates that FAK is involved in Rac1 activation and targeting, and that these two events occur in a similar time frame after integrin ligation.

After activation by specific GEFs, the Rho-family GTPase Rac1 promotes peripheral actin polymerization to induce the formation of lamellipodia and drive extension of the cell's leading edge (Hall, 2005). Membrane extension is made possible by Rac1 effects on peripheral F-actin organization.

Rac1 can induce Arp2/3 complex formation (Smith and Li, 2004), and this can be spatially focused by vinculin to sites of new focal adhesions (DeMali *et al.*, 2002). Formation of a stable lamellipodium in cells requires the activation and translocation of Rac to a subset of the cell perimeter (Ridley *et al.*, 1992; Burridge and Wennerberg, 2004). Recent data indicate that Rac targeting to the membrane edge is due at least in part to preferential binding to lipid rafts (del Pozo *et al.*, 2004). In addition to these positive targeting signals, Rac may also respond to negative molecular switches that reduce its activity in the trailing tails of migrating cells. Thus, the paxillin LD4 domain may mediate a reduction in Rac activity in these regions by recruiting an ADP-ribosylation factor GTPase-activating protein (Arf-GAP, e.g., GIT1 and/or PKL) that decreases Arf activity and inhibits Rac (Nishiya *et al.*, 2005). Our data demonstrate that Rac1 can precisely localize to focal adhesions and focal complexes at the leading edges of actively evolving membrane ruffles and lamellipodia. This localization does not appear to be restricted to areas occupied by lipid rafts (data not shown). Further, we document that the activation state of Rac1 may strongly affect its localization. This finding is consonant with the work of other investigators who have reported both that constitutively active Rac1 may be found in focal adhesions (Manser *et al.*, 1997), and that Rac inactivation is associated with its exclusion from the rear of polarized, motile fibroblasts (Nishiya *et al.*, 2005). Rac1-targeting to focal adhesions in FAK⁺ cells may, therefore, be partly dependent on Rac1 activation.

Interactions between FAK and Rac1 are incompletely understood. Our work demonstrates that FAK is involved in Rac1 activation and targeting, with subsequent positive effects on cell spreading. FAK has been implicated as an indirect actor in various Rac1 activation mechanisms. First, a p130CAS-Crk-DOCK180 complex can activate Rac1 in 293T cells (Kiyokawa *et al.*, 1998), and FAK may play a scaffolding role in the process of Src-mediated CAS phosphorylation (Ruest *et al.*, 2001). In another cascade in NIH3T3 cells, PI 3-kinase can stimulate the Rac-specific GEF activity in Vav2 by providing membrane targeting through phosphatidylinositol 3,4,5-trisphosphate (Das *et al.*, 2000). FAK activates PI 3-kinase after FAK Y³⁹⁷ interaction with the SH2 domain in the p85 regulatory subunit of PI 3-kinase (Chen and Guan, 1994; Chen *et al.*, 1996). Third, focal adhesion targeting of the paxillin-PKL- β PIX-PAK complex is dependent on tyrosine phosphorylation of p95PKL by FAK and Src in CHO.K1 cells (Brown *et al.*, 2005; ten Klooster *et al.*, 2006).

The third of these scenarios is most germane to the data presented in this current report. β PIX is an activator of Rac that associates with Rac1 in our activity assays and may target Rac1 to focal adhesions (ten Klooster *et al.*, 2006). Additionally, β PIX has been shown to play a key role in focal adhesion formation, cell migration, cell polarity, and cytoskeletal rearrangement. Recent studies have shown that disruption of PAK/PIX binding in the human breast cancer cell lines SK-BR-3 and ZR-75-1 altered cell-matrix adhesion and motility (Stofega *et al.*, 2004). In addition, overexpression of β PIX drives the formation of membrane ruffles via activation of Rac1, and it has been shown that LPA-induced cell motility in NIH-3T3 cells requires β PIX (Lee *et al.*, 2005). These observations strongly suggest that β PIX may accelerate leading edge extension.

Our studies suggest direct and specific roles for β PIX in FAK-mediated Rac1 targeting to focal adhesions and in FAK-facilitated cell spreading. We report that FAK associates with and tyrosine-phosphorylates β PIX and that this phosphorylation event is associated with an increased bind-

ing of β PIX to Rac1. An interaction between β PIX and FAK has also been demonstrated in NIH3T3 mouse fibroblasts (Lee *et al.*, 2005). Tyrosine phosphorylation has been shown to be an important regulatory event for other GEFs that are Rac-specific. For example, the activity of Vav is positively regulated by phosphorylation via the tyrosine kinase Lck (Han *et al.*, 1997). Ras-GRF1 has also been shown to be tyrosine-phosphorylated by Src (Kiyono *et al.*, 2000), and this induces its Rac-specific GEF activity.

Spatial regulation of β PIX has yet to be precisely defined. It is possible that FAK-dependent tyrosine phosphorylation of β PIX has a role in dynamic shuttling between cytoplasmic complexes, endosomal sequestration, and membrane targeting at ruffles and lamellipodial leading edges (Manabe *et al.*, 2002; Rosenberger and Kutsche, 2005). GIT1 and PKL may also be part of the β PIX trafficking between these various destinations (Manabe *et al.*, 2002; Brown *et al.*, 2005). Our observations that β PIX localizes to a subset of focal adhesions and that its presence at these sites may be challenging to document correlate well with the findings of other investigators (ten Klooster *et al.*, 2006; Wiggan *et al.*, 2006). It may therefore be reasonable to conclude at this juncture that direct binding to β PIX only partly accounts for Rac1 targeting to focal adhesions.

We propose a tripartite process that synthesizes our data on Rac1 activation and β PIX effects into a coherent model linking Rac1 and β PIX to focal adhesions. The three components of this model may go forward in the same time frame while mutually reinforcing one another. In the first component, adhesion-mediated activation of FAK is followed by FAK-mediated augmentation of β PIX-induced Rac1 activation. The second component of this model involves Rac1 targeting to focal adhesions. This targeting is favored by the interaction of β PIX with Rac1 that may be augmented by tyrosine phosphorylation of β PIX by FAK and by the specific intermolecular binding interaction that has just recently been described between the β PIX SH3 domain and the proline-rich sequence near the carboxy-terminus of Rac1 (ten Klooster *et al.*, 2006). Increased GTP loading of Rac1 may also favor targeting to focal adhesions. The third and final component of this proposed schema is that elevated levels of GTP loading on activated Rac1 may stabilize intermolecular interactions with its downstream effectors (del Pozo *et al.*, 2002). This effect would favor membrane extension and cell spreading.

The case for β PIX as a key player in FAK-facilitated lamellipodial extension and stability is made stronger by the aggregate of our findings: The GEF-deficient and PAK-binding incompetent β PIX-SH3/DH mutant antagonized Rac1 focal adhesion targeting and cell spreading efficiency in FAK+ cells, whereas wild-type β PIX rescued both of these processes in FAK- cells. The effectiveness of the β PIX-SH3/DH construct as a dominant negative reagent in our assays may be due in part to the abrogation of the function of key intermolecular complexes that incorporate β PIX, PAK, and Rac. We have observed dimerization of exogenous β PIX-Flag with native β PIX. Others have noted that this dimerization increases activation of, and specificity for the substrate Rac, whereas the PIX SH3 domain stabilizes the interaction of these dimers with both Rac and PAK (Feng *et al.*, 2002, 2004). We propose that the double mutant β PIX construct inhibits Rac-binding by these complexes, making the double mutant β PIX a more effective dominant negative than either of the single β PIX mutants in which either the DH or SH3 domain alone is defective.

Rescue of the FAK- phenotype for Rac1 targeting and cell spreading may be due to several alternative or complemen-

tary mechanisms. First, optimal β PIX GEF function is apparently dependent on both serine phosphorylation via PAK and tyrosine phosphorylation by FAK. If the size of the β PIX pool is a limiting factor for Rac1 activation and cell spreading, the elevation of β PIX availability in WT- β PIX-transfected FAK- cells may overcome the functional deficit from the lack of tyrosine phosphorylation and sufficiently boost Rac1 activation levels to restore cell spreading. It is also possible that the increased level of β PIX in these cells augments Rac1 recruitment to focal adhesions more efficiently and that this spatial focusing substantially increases the functional impact of the added β PIX expression on cell phenotype (ten Klooster *et al.*, 2006).

Finally, several critically important cellular behaviors require spatial focusing of Rac1 and directed, persistent extension of lamellipodia. These include fibroblast motility during wound repair and endothelial metamorphosis during angiogenesis (Cascone *et al.*, 2003; Harms *et al.*, 2005). The FAK- β PIX-Rac1 pathway that is defined in this work may be a critical determinant of success in these endeavors by providing the targeting and assembly of Rac1-containing molecular networks at focal complex and focal adhesion sites.

ACKNOWLEDGMENTS

We thank Denise Horvitz and Amy Kerman for technical assistance. We also extend special thanks to Steve Hanks for the FAK null and FAK reexpressing fibroblasts, to Michael Eck for the baculovirus-generated FAK kinase domain, to Peter Hordijk for the β PIX-GST, to Silvio Gutkind for the myristylated FAK, to Keith Burridge and Mike Schaller for valuable discussions, and to Patricia Arauz for comments on the manuscript. This work was supported by the National Institutes of Health (P60DE13079 and AI061042), the Fogarty International Center (F06TW02341), and the Johns Hopkins University Funds for Medical Discovery to L.R.

REFERENCES

- Arthur, W. T., Petch, L. A., and Burridge, K. (2000). Integrin engagement suppresses RhoA activity via a c-Src-dependent mechanism. *Curr. Biol.* 10, 719–722.
- Benard, V., Bohl, B. P., and Bokoch, G. M. (1999). Characterization of rac and cdc42 activation in chemoattractant-stimulated human neutrophils using a novel assay for active GTPases. *J. Biol. Chem.* 274, 13198–13204.
- Brown, M. C., Cary, L. A., Jamieson, J. S., Cooper, J. A., and Turner, C. E. (2005). Src and FAK kinases cooperate to phosphorylate paxillin kinase linker, stimulate its focal adhesion localization, and regulate cell spreading and protrusiveness. *Mol. Biol. Cell* 16, 4316–4628.
- Brown, M. C., West, K. A., and Turner, C. E. (2002). Paxillin-dependent paxillin kinase linker and p21-activated kinase localization to focal adhesions involves a multistep activation pathway. *Mol. Biol. Cell* 13, 1550–1565.
- Burridge, K., Turner, C. E., and Romer, L. H. (1992). Tyrosine phosphorylation of paxillin and pp125FAK accompanies cell adhesion to extracellular matrix: a role in cytoskeletal assembly. *J. Cell Biol.* 119, 893–903.
- Burridge, K., and Wennerberg, K. (2004). Rho and Rac take center stage. *Cell* 116, 167–179.
- Cascone, I., Giraudo, E., Caccavari, F., Napione, L., Bertotti, E., Collard, J. G., Serini, G., and Bussolino, F. (2003). Temporal and spatial modulation of Rho GTPases during in vitro formation of capillary vascular network. Adherens junctions and myosin light chain as targets of Rac1 and RhoA. *J. Biol. Chem.* 278, 50702–50713.
- Chen, B. H., Tzen, J. T., Bresnick, A. R., and Chen, H. C. (2002). Roles of Rho-associated kinase and myosin light chain kinase in morphological and migratory defects of focal adhesion kinase-null cells. *J. Biol. Chem.* 277, 33857–33863.
- Chen, H. C., Appeddu, P. A., Isoda, H., and Guan, J. L. (1996). Phosphorylation of tyrosine 397 in focal adhesion kinase is required for binding phosphatidylinositol 3-kinase. *J. Biol. Chem.* 271, 26329–26334.
- Chen, H. C., and Guan, J. L. (1994). Stimulation of phosphatidylinositol 3'-kinase association with focal adhesion kinase by platelet-derived growth factor. *J. Biol. Chem.* 269, 31229–31233.

- Clark, E. A., King, W. G., Brugge, J. S., Symons, M., and Hynes, R. O. (1998). Integrin-mediated signals regulated by members of the rho family of GTPases. *J. Cell Biol.* *142*, 573–586.
- Cooley, M. A., Broome, J. M., Ohngemach, C., Romer, L. H., and Schaller, M. D. (2000). Paxillin binding is not the sole determinant of focal adhesion localization or dominant-negative activity of focal adhesion kinase/focal adhesion kinase-related nonkinase. *Mol. Biol. Cell* *11*, 3247–3263.
- Das, B., Shu, X., Day, G. J., Han, J., Krishna, U. M., Falck, J. R., and Broek, D. (2000). Control of intramolecular interactions between the pleckstrin homology and Dbl homology domains of Vav and Sos1 regulates Rac binding. *J. Biol. Chem.* *275*, 15074–15081.
- del Pozo, M. A., Alderson, N. B., Kiosses, W. B., Chiang, H. H., Anderson, R. G., and Schwartz, M. A. (2004). Integrins regulate Rac targeting by internalization of membrane domains. *Science* *303*, 839–842.
- del Pozo, M. A., Kiosses, W. B., Alderson, N. B., Meller, N., Hahn, K. M., and Schwartz, M. A. (2002). Integrins regulate GTP-Rac localized effector interactions through dissociation of Rho-GDI. *Nat. Cell Biol.* *4*, 232–239.
- DeMali, K. A., Barlow, C. A., and Burridge, K. (2002). Recruitment of the Arp2/3 complex to vinculin: coupling membrane protrusion to matrix adhesion. *J. Cell Biol.* *159*, 881–891.
- Ezratty, E. J., Partridge, M. A., and Gundersen, G. G. (2005). Microtubule-induced focal adhesion disassembly is mediated by dynamin and focal adhesion kinase. *Nat. Cell Biol.* *7*, 581–590.
- Feng, Q., Albeck, J. G., Cerione, R. A., and Yang, W. (2002). Regulation of the Cool/Pix proteins: key binding partners of the Cdc42/Rac targets, the p21-activated kinases. *J. Biol. Chem.* *277*, 5644–5650.
- Feng, Q., Baird, D., and Cerione, R. A. (2004). Novel regulatory mechanisms for the Dbl family guanine nucleotide exchange factor Cool-2/ α -Pix. *EMBO J.* *23*, 3492–3504.
- Gu, J., Tamura, M., and Yamada, K. M. (1998). Tumor suppressor PTEN inhibits integrin- and growth factor-mediated mitogen-activated protein (MAP) kinase signaling pathways. *J. Cell Biol.* *143*, 1375–1383.
- Hall, A. (2005). Rho GTPases and the control of cell behaviour. *Biochem. Soc. Trans.* *33*, 891–895.
- Han, J., Das, B., Wei, W., Van Aelst, L., Mosteller, R. D., Khosravi-Far, R., Westwick, J. K., Der, C. J., and Broek, D. (1997). Lck regulates Vav activation of members of the Rho family of GTPases. *Mol. Cell Biol.* *17*, 1346–1353.
- Hanks, S. K., Calalb, M. B., Harper, M. C., and Patel, S. K. (1992). Focal adhesion protein-tyrosine kinase phosphorylated in response to cell attachment to fibronectin. *Proc. Natl. Acad. Sci. USA* *89*, 8487–8491.
- Harms, B. D., Bassi, G. M., Horwitz, A. R., and Lauffenburger, D. A. (2005). Directional persistence of EGF-induced cell migration is associated with stabilization of lamellipodial protrusions. *Biophys. J.* *88*, 1479–1488.
- Holinstat, M., Knezevic, N., Broman, M., Samarel, A. M., Malik, A. B., and Mehta, D. (2006). Suppression of RhoA activity by focal adhesion kinase-induced activation of p190RhoGAP: role in regulation of endothelial permeability. *J. Biol. Chem.* *281*, 2296–2305.
- Hsia, D. A., *et al.* (2003). Differential regulation of cell motility and invasion by FAK. *J. Cell Biol.* *160*, 753–767.
- Ilic, D., Furuta, Y., Kanazawa, S., Takeda, N., Sobue, K., Nakatsuji, N., Nomura, S., Fujimoto, J., Okada, M., and Yamamoto, T. (1995). Reduced cell motility and enhanced focal adhesion contact formation in cells from FAK-deficient mice. *Nature* *377*, 539–544.
- Kiyokawa, E., Hashimoto, Y., Kobayashi, S., Sugimura, H., Kurata, T., and Matsuda, M. (1998). Activation of Rac1 by a Crk SH3-binding protein, DOCK180. *Genes Dev.* *12*, 3331–3336.
- Kiyono, M., Kaziro, Y., and Satoh, T. (2000). Induction of rac-guanine nucleotide exchange activity of Ras-GRF1/CDC25(Mm) following phosphorylation by the nonreceptor tyrosine kinase Src. *J. Biol. Chem.* *275*, 5441–5446.
- Laemmli, U. K., Beguin, F., and Gujer-Kellenberger, G. (1970). A factor preventing the major head protein of bacteriophage T4 from random aggregation. *J. Mol. Biol.* *47*, 69–85.
- Lee, J., *et al.* (2005). p85 beta-PIX is required for cell motility through phosphorylations of focal adhesion kinase and p38 MAP kinase. *Exp. Cell Res.* *307*, 315–328.
- Machesky, L. M., and Hall, A. (1997). Role of actin polymerization and adhesion to extracellular matrix in Rac- and Rho-induced cytoskeletal reorganization. *J. Cell Biol.* *138*, 913–926.
- Manabe, R., Kovalenko, M., Webb, D. J., and Horwitz, A. R. (2002). GIT1 functions in a motile, multi-molecular signaling complex that regulates protrusive activity and cell migration. *J. Cell Sci.* *115*, 1497–1510.
- Manser, E., Huang, H. Y., Loo, T. H., Chen, X. Q., Dong, J. M., Leung, T., and Lim, L. (1997). Expression of constitutively active alpha-PAK reveals effects of the kinase on actin and focal complexes. *Mol. Cell Biol.* *17*, 1129–1143.
- Manser, E., Loo, T. H., Koh, C. G., Zhao, Z. S., Chen, X. Q., Tan, L., Tan, L., Leung, T., and Lim, L. (1998). PAK kinases are directly coupled to the PIX family of nucleotide exchange factors. *Mol. Cell* *1*, 183–192.
- Nishiya, N., Kiosses, W. B., Han, J., and Ginsberg, M. H. (2005). An alpha4 integrin-paxillin-Arf-GAP complex restricts Rac activation to the leading edge of migrating cells. *Nat. Cell Biol.* *7*, 343–352.
- Nobes, C. D., and Hall, A. (1999). Rho GTPases control polarity, protrusion, and adhesion during cell movement. *J. Cell Biol.* *144*, 1235–1244.
- Owen, J. D., Ruest, P. J., Fry, D. W., and Hanks, S. K. (1999). Induced focal adhesion kinase (FAK) expression in FAK-null cells enhances cell spreading and migration requiring both auto- and activation loop phosphorylation sites and inhibits adhesion-dependent tyrosine phosphorylation of Pyk2. *Mol. Cell Biol.* *19*, 4806–4818.
- Prutzman, K. C., Gao, G., King, M. L., Iyer, V. V., Mueller, G. A., Schaller, M. D., and Campbell, S. L. (2004). The focal adhesion targeting domain of focal adhesion kinase contains a hinge region that modulates tyrosine 926 phosphorylation. *Structure* *12*, 881–891.
- Ren, X. D., Kiosses, W. B., and Schwartz, M. A. (1999). Regulation of the small GTP-binding protein Rho by cell adhesion and the cytoskeleton. *EMBO J.* *18*, 578–585.
- Ren, X. D., Kiosses, W. B., Sieg, D. J., Otey, C. A., Schlaepfer, D. D., and Schwartz, M. A. (2000). Focal adhesion kinase suppresses Rho activity to promote focal adhesion turnover. *J. Cell Sci.* *113*, 3673–3678.
- Richardson, A., Malik, R. K., Hildebrand, J. D., and Parsons, J. T. (1997). Inhibition of cell spreading by expression of the C-terminal domain of focal adhesion kinase (FAK) is rescued by coexpression of Src or catalytically inactive FAK: a role for paxillin tyrosine phosphorylation. *Mol. Cell Biol.* *17*, 6906–6914.
- Richardson, A., and Parsons, T. (1996). A mechanism for regulation of the adhesion-associated protein tyrosine kinase pp125FAK. *Nature* *380*, 538–540.
- Ridley, A. J., Paterson, H. F., Johnston, C. L., Diekmann, D., and Hall, A. (1992). The small GTP-binding protein rac regulates growth factor-induced membrane ruffling. *Cell* *70*, 401–410.
- Romer, L. H., Birukov, K. G., and Garcia, J. G. (2006). The focal adhesions: paradigm for a signaling nexus. *Circ. Res.* *98*, 606–616.
- Rosenberger, G., and Kutsche, K. (2005). alphaPIX and betaPIX and their role in focal adhesion formation. *Eur. J. Cell Biol.* *85*, 265–274.
- Ruest, P. J., Roy, S., Shi, E., Mernaugh, R. L., and Hanks, S. K. (2000). Phosphospecific antibodies reveal focal adhesion kinase activation loop phosphorylation in nascent and mature focal adhesions and requirement for the autophosphorylation site. *Cell Growth Differ.* *11*, 41–48.
- Ruest, P. J., Shin, N. Y., Polte, T. R., Zhang, X., and Hanks, S. K. (2001). Mechanisms of CAS substrate domain tyrosine phosphorylation by FAK and Src. *Mol. Cell Biol.* *21*, 7641–7652.
- Schaller, M. D. (2001). Biochemical signals and biological responses elicited by the focal adhesion kinase. *Biochim. Biophys. Acta* *1540*, 1–21.
- Schaller, M. D., Borgman, C. A., Cobb, B. S., Vines, R. R., Reynolds, A. B., and Parsons, J. T. (1992). pp125FAK a structurally distinctive protein-tyrosine kinase associated with focal adhesions. *Proc. Natl. Acad. Sci. USA* *89*, 5192–5196.
- Schaller, M. D., and Parsons, J. T. (1995). pp125FAK-dependent tyrosine phosphorylation of paxillin creates a high-affinity binding site for Crk. *Mol. Cell Biol.* *15*, 2635–2645.
- Schlaepfer, D. D., Broome, M. A., and Hunter, T. (1997). Fibronectin-stimulated signaling from a focal adhesion kinase-c-Src complex: involvement of the Grb2, p130cas, and Nck adaptor proteins. *Mol. Cell Biol.* *17*, 1702–1713.
- Schlaepfer, D. D., Hauck, C. R., and Sieg, D. J. (1999). Signaling through focal adhesion kinase. *Prog. Biophys. Mol. Biol.* *71*, 435–478.
- Shin, E. Y., *et al.* (2002). Phosphorylation of p85 beta PIX, a Rac/Cdc42-specific guanine nucleotide exchange factor, via the Ras/ERK/PAK2 pathway is required for basic fibroblast growth factor-induced neurite outgrowth. *J. Biol. Chem.* *277*, 44417–44430.
- Shin, E. Y., Woo, K. N., Lee, C. S., Koo, S. H., Kim, Y. G., Kim, W. J., Bae, C. D., Chang, S. I., and Kim, E. G. (2004). Basic fibroblast growth factor stimulates activation of Rac1 through a p85 betaPIX phosphorylation-dependent pathway. *J. Biol. Chem.* *279*, 1994–2004.
- Sieg, D. J., Hauck, C. R., and Schlaepfer, D. D. (1999). Required role of focal adhesion kinase (FAK) for integrin-stimulated cell migration. *J. Cell Sci.* *112*, 2677–2691.

- Smith, L. G., and Li, R. (2004). Actin polymerization: riding the wave. *Curr. Biol.* *14*, R109–R111.
- Stofega, M. R., Sanders, L. C., Gardiner, E. M., and Bokoch, G. M. (2004). Constitutive p21-activated kinase (PAK) activation in breast cancer cells as a result of mislocalization of PAK to focal adhesions. *Mol. Biol. Cell* *15*, 2965–2977.
- Takahashi, N., Seko, Y., Noiri, E., Tobe, K., Kadowaki, T., Sabe, H., and Yazaki, Y. (1999). Vascular endothelial growth factor induces activation and subcellular translocation of focal adhesion kinase (p125FAK) in cultured rat cardiac myocytes. *Circ. Res.* *84*, 1194–1202.
- ten Klooster, J. P., Jaffer, Z. M., Chernoff, J., and Hordijk, P. L. (2006). Targeting and activation of Rac1 are mediated by the exchange factor β -Pix. *J. Cell Biol.* *172*, 759–769.
- Thomas, J. W., Cooley, M. A., Broome, J. M., Salgia, R., Griffin, J. D., Lombardo, C. R., and Schaller, M. D. (1999). The role of focal adhesion kinase binding in the regulation of tyrosine phosphorylation of paxillin. *J. Biol. Chem.* *274*, 36684–36692.
- Towbin, H., Staehelin, T., and Gordon, J. (1979). Electrophoretic transfer of proteins from polyacrylamide gels to nitrocellulose sheets: procedure and some applications. *Proc. Natl. Acad. Sci. USA* *76*, 4350–4354.
- Turner, C. E. (2000). Paxillin interactions. *J. Cell Sci.* *113*, 4139–4140.
- Turner, C. E., Brown, M. C., Perrotta, J. A., Riedy, M. C., Nikolopoulos, S. N., McDonald, A. R., Bagrodia, S., Thomas, S., and Leventhal, P. S. (1999). Paxillin LD4 motif binds PAK and PIX through a novel 95-kD ankyrin repeat, ARF-GAP protein: a role in cytoskeletal remodeling. *J. Cell Biol.* *145*, 851–863.
- West, K. A., Zhang, H., Brown, M. C., Nikolopoulos, S. N., Riedy, M. C., Horwitz, A. F., and Turner, C. E. (2001). The LD4 motif of paxillin regulates cell spreading and motility through an interaction with paxillin kinase linker (PKL). *J. Cell Biol.* *154*, 161–176.
- Wiggin, O., Shaw, A. E., and Bamburg, J. R. (2006). Essential requirement for Rho family GTPase signaling in Pax3 induced mesenchymal-epithelial transition. *Cell Signal.* *18*, 1501–1514.
- Yu, D. H., Qu, C. K., Henegariu, O., Lu, X., and Feng, G. S. (1998). Protein-tyrosine phosphatase Shp-2 regulates cell spreading, migration, and focal adhesion. *J. Biol. Chem.* *273*, 21125–21131.
- Zhao, Z. S., Manser, E., Loo, T. H., and Lim, L. (2000). Coupling of PAK-interacting exchange factor PIX to GIT1 promotes focal complex disassembly. *Mol. Cell. Biol.* *20*, 6354–6363.